

# Structure of $c(4 \times 2)$ Superlattice in Alkanethiolate Self-Assembled Monolayers

Reena Bhatia and Barbara J. Garrison\*

Department of Chemistry, The Pennsylvania State University,  
University Park, Pennsylvania 16802

Received December 2, 1996. In Final Form: May 22, 1997<sup>⊗</sup>

Molecular dynamic simulations have been used to elucidate the  $c(4 \times 2)$  superlattice structure of  $\text{CH}_3\text{-(CH}_2\text{)}_{n-1}\text{S-}$  chains self-assembled on  $\text{Au}\{111\}$ . This superlattice of a  $(\sqrt{3} \times \sqrt{3})\text{R}30^\circ$  overlayer has been observed in several experimental studies. Using experimental clues as guidelines, a systematic study of the phase-space of the orientations of the chain backbones and their directions of tilt has been performed. Three possible structures for monolayers formed from long chains ( $n \geq 12$ ) and one for short ones ( $n = 4, 6$ ) all of which are consistent with the symmetry suggested by X-ray diffraction experiments are identified. Two of the four structures proposed show the same surface topology as predicted by scanning tunneling microscopy. The simulations also show that a complex interplay exists among the azimuthal tilt direction, the polar tilt angle, and the chain backbone orientation.

## INTRODUCTION

The  $c(4 \times 2)$  superlattice is one of the two commonly observed superlattices of a basic  $(\sqrt{3} \times \sqrt{3})\text{R}30^\circ$  monolayer of alkanethiolate chains self-assembled on  $\text{Au}\{111\}$ . Although several characteristics have been identified, the full description of the structure is still not known. Self-assembled monolayers (SAMs) have tremendous technological potential,<sup>1,2</sup> and it is desirable to have a complete understanding of its structure in order to help realize this potential. Molecular dynamics is a useful approach that can provide valuable insights in elucidating the structure as one can look for stable low-energy structures that replicate the features observed experimentally.

All experiments performed to date suggest that the monolayers consist of more than one kind of orientation of the chain backbones. Poirier and Tarlov have performed scanning tunneling microscopy (STM) measurements<sup>3</sup> that clearly show that the surface of these monolayers exhibit a repeating pattern of bright and dark spots that correspond to a  $c(4 \times 2)$  superlattice of a basic  $(\sqrt{3} \times \sqrt{3})\text{R}30^\circ$  overlayer. IR reflectance spectroscopy<sup>4</sup> shows a split in the absorption peak corresponding to the methylene scissor vibrational mode. This feature is characteristic of bulk alkanes which have a herringbone arrangement<sup>5</sup> with the carbon backbones of the adjacent chains perpendicular to one another. X-ray diffraction studies by Fenter and Eisenberger<sup>6</sup> on monolayers of 10-carbon chains show missing peaks characteristic of a rectangular symmetry. They also see half-integral peaks that arise from the Au/S interface region and deduce that the rectangular symmetry is characteristic of not only the carbon backbones but also the sulfur headgroups and the gold atoms that comprise the interface.

Computer simulations have also been performed to get a better understanding of the microscopic structure of these monolayers. Mar and Klein<sup>7</sup> used molecular dynamics to study the relative stability of several two-chain and four-chain unit cell structures. They compared the energies of these configurations and concluded that a two-

chain per unit cell herringbone arrangement is favored over that of four-chain per unit cell arrangements. The gold substrate used was rigid, however, and the sulfur headgroup positions were artificially constrained by making use of a large van der Waal radius for the sulfur atoms. Gerdy and Goddard<sup>8</sup> used force fields based on quantum mechanics to propose a structure following calculations on dodecanethiol dimers assembled on  $\text{Au}\{111\}$ . These authors assumed that the sulfur headgroups exist as dimers following predictions from X-ray diffraction experiments performed by Fenter and Eisenberger on monolayers of 10-carbon chains.<sup>6</sup> Pertsin and Grunze used four all-atom chain models, a rigid but corrugated surface, and a Au–S–C angle bend interaction.<sup>9</sup> They performed a random search over configuration space and minimized the energy of the system. They found for all four all-atom potentials that only one and two chains per unit cell arrangements are the most stable. They conclude “a discouraging result of this work is that neither of the four forcefields used in the calculations predicts a four chain unit cell structure to be the most stable one.” The approach used in our work is different from the above mentioned investigations, namely, the sulfur headgroups are mobile on a moving  $\text{Au}\{111\}$  substrate and no assumptions are made regarding the existence of sulfurs as dimers. Rather, we look for any tendencies in the sulfur headgroups to move out of their  $(\sqrt{3} \times \sqrt{3})\text{R}30^\circ$  sites.

In order to deduce the underlying structure of the  $c(4 \times 2)$  superlattice, it is important to understand that several factors play a role in determining the structural characteristics of a molecular monolayer. The structure of a monolayer is a result of competing chain–substrate and chain–chain interactions. The latter depends on chain length so there might exist at least slightly, if not totally, different structures for similar monolayers composed of different chain lengths. Indeed, Fenter and Eisenberger<sup>10,11</sup> see two different regimes of chain lengths ( $10 \leq n \leq 14$  and  $16 \leq n \leq 30$ ), each showing a different preference for tilt angle with respect to the surface normal and the direction of tilt with respect to the neighboring chains. Consequently, there may be several structures that correspond to the  $c(4 \times 2)$  superlattice.

<sup>⊗</sup> Abstract published in *Advance ACS Abstracts*, July 1, 1997.

(1) Ulman, A. *Chem. Rev.* **1996**, *96*, 1553.  
(2) Allara, D. L. *Biosens. Bioelectron.* **1995**, *10*, 771.  
(3) Poirier, G. E.; Tarlov, M. J. *Langmuir* **1994**, *10*, 2853.  
(4) Nuzzo, R. G.; Korenic, E. M.; Dubois L. H. *J. Chem. Phys.* **1990**, *93*, 767.  
(5) Snyder, R. G. *J. Chem. Phys.* **1979**, *71*, 3229.  
(6) Fenter, P.; Eberhardt, A.; Eisenberger, P. *Science* **1994**, *266*, 1216.  
(7) Mar, W.; Klein, M. L. *Langmuir* **1994**, *10*, 188.

(8) Gerdy, J. J.; Goddard, W. A. *J. Am. Chem. Soc.* **1996**, *118*, 3223.  
(9) Pertsin, A. J.; Grunze, M. *Langmuir* **1994**, *10*, 3668.  
(10) Fenter, P. Private communication.  
(11) Fenter, P.; Eisenberger, P.; Liang, K. S. *Phys. Rev. Lett.* **1993**, *70*, 2247.

Temperature also plays a significant role in the determination of the monolayer structure. At high temperatures, the packing of the chains can be influenced by entropic factors that can favor configurations which do not correspond to the minimum energy (enthalpy) configuration. In fact, Langmuir monolayers assembled on water exhibit a rich phase behavior that shows the chains choosing different tilt directions depending on the temperature.<sup>12</sup> We have recently reported similar behavior in alkanethiolate monolayers self-assembled on Au{111}.<sup>13</sup>

Given the possibility of more than one structure, it is desirable to find several structures that are consistent with the experimental data. We have used molecular dynamics to do an exhaustive search of the whole phase space of chain orientations and tilt directions to come up with possible candidates for the  $c(4 \times 2)$  superlattice. Four structures, three for long chains ( $n \geq 12$ ) and one for short chains ( $n = 4, 6$ ), are proposed.

### Computational Method

The complexity in the phase behavior of molecular monolayers makes molecular dynamics a suitable method for studying their structural characteristics as one can sample any part of the overall phase space. In order to find a vast array of local minima, a systematic study of all possible orientations of the chain backbones and the monolayer tilt directions is carried out. In this study, the chains are placed in a variety of configurations that map a grid in phase-space and are then tested for their stability and/or their ability to replicate experimental features. Below we give the system used, the potentials used to describe the system, the selection of starting configurations, and the criteria used to accept or reject a given configuration.

The system used consists of 64 chains forming a  $(\sqrt{3} \times \sqrt{3})R30^\circ$  overlayer over eight layers of Au atoms containing 192 atoms each. The top three Au layers are allowed to move according to Newton's equations of motion. The bottom-most layer of the slab is kept rigid to hold the crystal in place. The remaining four intermediate layers are treated as a heat-bath using the generalized Langevin equations (GLE)<sup>14</sup> so the whole system could be maintained at a desired temperature. The GLE method allows one to control the temperatures using the metal atoms several angstroms away from the molecules of interest, thus not directly altering the trajectories of the organic film as happens with the velocity rescaling approach. The  $\text{CH}_x$  units comprising the chains are treated within the united-atom limit, and the potentials used to describe the inter- and intrachain forces are given by Hautman and Klein<sup>15</sup> where we used the smallest of the S-S interaction in their Table II. The bonds connecting the  $\text{CH}_x$  units are kept at a fixed length using the RATTLE algorithm.<sup>16</sup> We developed the potentials used to describe the interface and the substrate-chain interactions. For the Au-S interactions, we use a Morse potential fit to parameters obtained from quantum mechanical calculations by Sellers<sup>17</sup> and for the Au- $\text{CH}_x$  interactions we use a 12-6 Lennard-Jones. The Au atoms are described by the many-body MD/MC corrected effective medium potentials de-

veloped by De Pristo *et al.*<sup>18-20</sup> The details of all the potentials used and their specific values can be found in ref 21. All Lennard-Jones potentials are cut off at 2.5 times the equilibrium distance. The sulfur headgroups are allowed to move freely on the gold surface, which is also mobile. The freedom of motion of the atoms comprising the Au/S interface allows for extra degrees of freedom that might be necessary in order to stabilize some configurations.

The validity of united atom potentials for simulations of SAMs has been questioned.<sup>7,22</sup> This conclusion is based on the observation that a stable next-nearest neighbor (NNN) structure could not be obtained. These studies, however, effectively fixed the S atoms in place and had a rigid, flat substrate. On the other hand, using a moving substrate and S atoms, we have shown that the united atom description can predict a stable NNN configuration at room temperature.<sup>13</sup> Thus it is not clear that the united atom potentials are inadequate to simulate SAMs. There are also numerous all-atom potentials in the literature.<sup>23</sup> To our knowledge, an exhaustive study has not been made of all the potentials with a moving substrate and the results from the simulation compared with detailed experimental data. Such comparisons have been made for other systems such as has recently been performed for liquid alkanes<sup>24</sup> and for Si.<sup>25</sup> In conclusion, we do not find in the literature overwhelming evidence that all-atom potentials are absolutely necessary to describe SAMs. We do believe, though, that moving surfaces are important as the barriers to diffusion are quite small.<sup>26</sup> We thus use the united atom potentials with a moving surface for the large phase space search for  $c(4 \times 2)$  structures as outlined in the following paragraph.

The nearest three neighboring shells, namely, the nearest neighbor (NN), the next-nearest neighbor (NNN), and the next-next-nearest neighbor (NNNN), most influence the interactions between a given chain and its neighbors. These neighbors are spaced  $15^\circ$  apart and so  $15^\circ$  intervals are chosen to cover the whole phase space of tilt directions and carbon backbone orientations. Figure 1 shows all the NN, NNN, and NNNN directions that are analyzed to perform the search for the  $c(4 \times 2)$  structural candidates. The symmetry suggested by the X-ray diffraction experiments<sup>6</sup> requires a four-chain unit cell with two types of chains whose carbon backbones are oriented differently from one another. To select a configuration, hence, we choose one orientation for the carbon backbones of chain type 1 and another for chain type 2, both of which are picked from the set of directions shown in Figure 1. For any given configuration, all possible directions of tilt (again, from the set of directions shown) with the same  $15^\circ$  intervals are tried. This is done until the whole phase space is analyzed. Figure 1 shows all of these 24 directions

(18) Stave, M. S.; Sanders, D. S.; Raeker, T. J.; DePristo, A. E. *J. Chem. Phys.* **1990**, *93*, 4413.

(19) Raeker, T. J.; Depristo, A. E. *Int. Rev. Phys. Chem.* **1991**, *10*, 1.  
(20) Kelchner, C. L.; Halstead, D. M.; Perkins, L. S.; Wallace, N. M.; DePristo, A. E. *Surf. Sci.* **1994**, *310*, 425.

(21) Mahaffy, R.; Bhatia, R.; Garrison, B. J. *J. Phys. Chem.* **1997**, *101*, 771.

(22) Bareman, J. P.; Klein, M. L. *J. Phys. Chem.* **1990**, *94*, 5202.

(23) For starters there are eight different all-atom potentials in Williams, D. E. *J. Chem. Phys.* **1967**, *47*, 4680; another one used in ref 8; and three recently developed for liquids: (a) Cornell, W. D.; Cieplak, P.; Bayly, C. L.; Gould, I. R.; Merz, K. M., Jr.; Ferguson, D. M.; Spellmeyer, D. C.; Fox, T.; Caldwell, J. W.; Kollman, P. A. *J. Am. Chem. Soc.* **1995**, *117*, 5179. (b) Halgren, T. A. *J. Comput. Chem.* **1996**, *17*, 490, 520, 553, 616. (c) Jorgensen, W. L.; Maxwell, D. S.; Tirado-Rives, J. *J. Am. Chem. Soc.* **1996**, *118*, 11225.

(24) Kaminski, G.; Jorgensen, W. L. *J. Phys. Chem.* **1996**, *100*, 18010.  
(25) Balamane, H.; Halicioglu, T.; Tiller, W. A. *Phys. Rev. B* **1992**, *46*, 2250.

(26) Beardmore, K. M.; Kress, J. D.; Grønbech-Jensen, N.; Bishop, A. R. Submitted to *Phys. Rev. Lett.*

(12) Lin, B.; Shih, M. C.; Bohanon, T. M.; Ice, G. E.; Dutta, P. *Phys. Rev. Lett.* **1990**, *65*, 191.

(13) Bhatia, R.; Garrison, B. J. *Langmuir* **1997**, *13*, 765.

(14) Garrison, B. J.; Kodali, P. B. S.; Srivastava, S. *Chem. Rev.* **1996**, *96*, 1327 and references therein.

(15) Hautman, J.; Klein, M. L. *J. Chem. Phys.* **1989**, *91*, 4994.

(16) Anderson, H. C. *J. Comput. Phys.* **1983**, *52*, 24.

(17) Sellers, H.; Ulman, A.; Shnidman, Y.; Eilers, J. E. *J. Am. Chem. Soc.* **1993**, *115*, 9389.

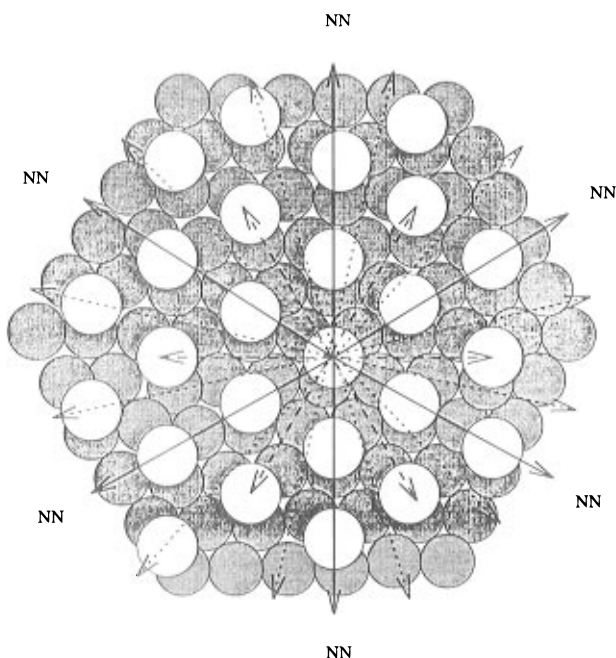


**Figure 1.** The Au/S interface showing the different NN, NNN, and NNNN directions considered for collective monolayer tilts and the backbone orientations of the two kinds of chains. The solid lines show the NN direction, the dashed lines the NNN direction, and the dotted lines the NNNN direction. The gray circles represent the first layer gold atoms and the white circles represent the sulfur headgroups.

that are used to pick the orientation of the backbones for the two kinds of chains and the collective tilt of the monolayer. The total number of configurations tested amounts to much less than the complete set of  $24^3$  possibilities as many of the configurations have equivalent counterparts. For example, for certain choices of chain orientations, it is sufficient for the tilt direction to span just two of the four quadrants.

The starting configuration consists of the two kinds of chains arranged to form a  $(\sqrt{3} \times \sqrt{3})R30^\circ$  overlayer such that they form a four-chain unit cell corresponding to the rectangular symmetry predicted by X-ray diffraction. As explained above, the tilt direction of the monolayer is chosen from the same set of directions shown in Figure 1. The initial polar tilt with respect to the surface normal is assigned to be  $30^\circ$  for all the cases, as all experimental studies on SAMs report values within a few degrees of this number. The temperature of the monolayer is chosen to be 100 K, although constant-energy runs are also performed. Since all three possible orientations (NN, NNN, NNNN) are being tested, higher initial temperatures (200 and 300 K) were often tried in order to take into account the fact that the chains undergo an orientational phase transition below room temperature.<sup>13</sup> The chosen configuration is allowed to run for varying lengths of time depending on the stability of the structure under consideration. The whole phase-space is examined for  $\text{CH}_3(\text{CH}_2)_{11}\text{S}-$  chains, but all the promising cases were repeated for shorter ( $n = 4, 6$ ) and longer ( $n \leq 20$ ) chains.

Several criteria are used to decide whether or not a structure is a good candidate for the  $c(4 \times 2)$  superlattice. None of the configurations satisfied all the criteria for acceptance, thus in each case some condition(s) had to be relaxed in order to obtain a few good structures. We discuss below each of the criteria used, the computational details involved when comparing to experimentally observed features, and the conditions under which the criterion could be relaxed.

First, the configuration, while it is stable, is required to maintain the original symmetry. To check for this, a qualitative diffraction pattern is computed and compared with that obtained experimentally.<sup>6</sup> The intensity,  $I$ , of any  $hkl$  reflection, depends on the relative positions of the atoms comprising a unit cell and can be calculated as follows<sup>27</sup>

$$I = [f_1 \cos 2\pi(hu_1 + kv_1 + lw_1) + f_2 \cos 2\pi(hu_2 + kv_2 + lw_2) + \dots]^2 + [f_1 \sin 2\pi(hu_1 + kv_1 + lw_1) + f_2 \sin 2\pi(hu_2 + kv_2 + lw_2) + \dots]^2$$

where, the unit cell contains atoms 1, 2, 3, ...,  $N$ , with fractional coordinates  $u_1, v_1, w_1, u_2, v_2, w_2, \dots, u_N, v_N, w_N$ , and atomic scattering factors  $f_1, f_2, f_3, \dots, f_N$ . The atomic scattering factor for the sulfur headgroups and the carbons composing the backbones were taken to be equal to their atomic number ( $f_C = 6; f_S = 16$ ). The contribution due to the Au atoms, however, was ignored. The two-dimensional projection of the diffraction pattern is obtained by setting  $l = 0$ . The experimentally observed diffraction pattern shows missing peaks characteristic of a rectangular symmetry in addition to some half-integral peaks that arise from the interface. All the diffraction patterns computed are required to show the missing peaks, else they are rejected. The half-integral peaks, however, are difficult to verify as the real motion of the sulfurs takes place at higher temperatures (200 K and above) and the potentials are not sufficiently repulsive to maintain a given structure when the temperature is raised such that the S atoms move significantly.

The second criterion for judging a candidate involved obtaining the topological map of the SAM surface and comparing it with the pictures observed by STM.<sup>3</sup> To generate the topological map, an imaginary point tip is brought close to the surface and the height where it first feels the van der Waal radius of any of the surface atoms is recorded. The procedure is repeated horizontally in two directions until the whole surface of the monolayer has been rastered. Although nonexistence of the STM topology is not a criterion for the rejection of a structure, those showing such patterns are taken seriously. It is beyond the scope of this work to discuss the physics behind STM pictures. Rather we use a simplistic definition of height variation to monitor our structures.

The relative energy of a given configuration was chosen as the third useful criterion in judging the candidates. Although we do not specifically look for the minimum energy configurations, the lower energy candidates are favored and those with very high energies are rejected. The time taken for the backbone orientations to deviate from their initial configurations is a strong indicator of their stability. The very high energy structures take only a few time steps to lose the symmetry whereas the low energy structures can take a while. Those that are very stable with respect to time are also reported as possible candidates. The long time survival condition, although important, is often relaxed, when a configuration showed the STM pattern and/or is very low in energy. This is because it is possible for the structure to survive for a different chain length due to different inter chain interactions or at another temperature range where the entropic contributions are different.

### Structures

Four structures for the  $c(4 \times 2)$  superlattice, one for the very short chains ( $n = 4, 6$ ) and three for the long ones

(27) Cullity, B. D. *Elements of X-ray Diffraction*; Addison-Wesley Publishing Co., Inc.: Reading, MA, 1978.

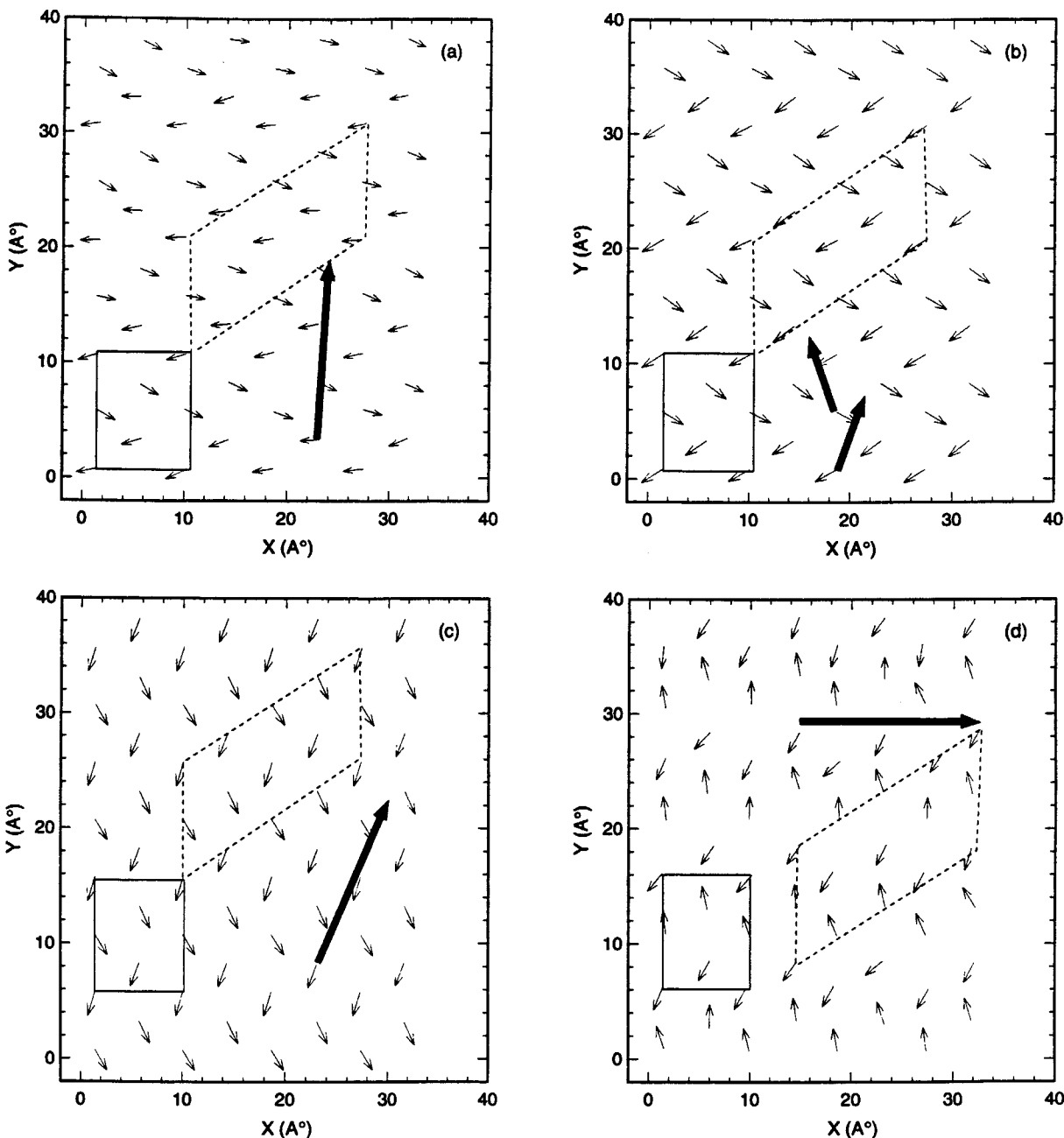


**Figure 2.** The four proposed structures for the  $c(4 \times 2)$  superlattice. Structures (a), (c), and (d) are for long chains ( $n \geq 12$ ) and (b) is for short ones ( $n = 4, 6$ ). The vectors represent the carbon backbone of the two kinds of chains and the bold arrows represent the collective tilt of the monolayer. The rectangles (solid lines) drawn depict the rectangular unit cell consistent with the electron diffraction study predictions. The parallelograms also depict the  $c(4 \times 2)$  cell containing eight chains. These  $c(4 \times 2)$  cells (dashed lines) for structures 2c and 2d correspond to those shown in the topological patterns in Figure 4 and Figure 5, respectively.

( $n \geq 12$ ) are proposed. Figure 2 shows these four structures with the two-dimensional vectors representing the plane of the chains and the bold arrows representing the average tilt direction of the whole monolayer. Each vector represents the projection of the plane containing the carbon backbone of a chain and is perpendicular to the chain axis. The tail ends of the vectors are placed at the sulfur headgroup position of the corresponding chain. The method of calculation of the vector components is exactly the same as that used by Hautman and Klein<sup>15</sup> to evaluate the " $R_a$ " parameter to estimate the deviation of a chain from an all-trans conformation. Specifically, the vector represents the average of the bisectors of the CCC angles with alternating signs normalized with respect to the value obtained for an all-trans chain. This  $R_a$  parameter lies in the plane of the carbon backbone, and we use the negative of this vector to represent the

orientation of a chain. Figure 3 shows a schematic of one chain with the arrow representing its carbon backbone placed at the position of the sulfur headgroup. The collective tilt directions of the monolayer (bold arrows) are approximate as they vary slightly with temperature and the degree of repulsiveness of the interchain van der Waals potentials.

It is immediately apparent from Figure 2 that none of the four structures assumes the perfectly perpendicular herringbone arrangement as depicted in most experimental and theoretical papers. The main reason for this popular belief is that in bulk alkanes the backbones of the adjacent chains are known to be perpendicular to one another<sup>5</sup> and self-assembled monolayers show similar IR spectral behavior characteristic of this arrangement. In all the configurations examined, the chain backbones always seem to prefer orienting such that they point

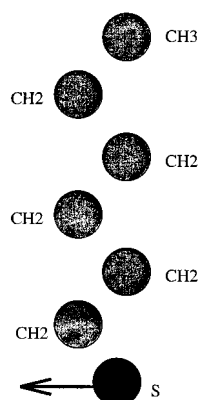


**Figure 3.** A schematic illustration of the placement of the vector representing the carbon backbone of the chain that lies in its CCC plane.

toward one of the three neighboring shells instead of orienting at an angle of  $90^\circ$  with respect to another neighboring chain backbone. Consequently, the two kinds of chains assume a “skewed” herringbone arrangement with the interplanar angle usually very different from  $90^\circ$ . Since the two kinds of backbones are still nonlinear in all the structures shown, it is possible that these arrangements are still consistent with the IR spectral behavior.

Given two kinds of chains, the backbones or the vectors representing them can either face each other or be oriented such that the arrow-head of one points toward the tail-end of another. In that sense, structures 2a, 2b, and 2c have very similar relative orientation of the two kinds of chains, but the differences in the preferred tilt direction make them very distinct from one another.

Only two of the proposed structures, namely, structures 2a and 2b, are stable with respect to time at lower temperatures ( $\leq 100$  K). The structures 2c and 2d are “partially” stable in the sense that they survive several hundred timesteps before the chains reorient themselves resulting in loss of the structure. The tilt directions depicted for these two structures are approximate to within  $\pm 15^\circ$  beyond which the chain backbones tend to reorient. Structures 2a and 2b have their collective tilts closer to the NN direction and structures 2c and 2d show monolayer tilts in a non-NN direction. In our earlier work on temperature-dependent behavior of self-assembled monolayers, we have shown that the chains prefer a NN orientation at low temperatures and undergo a phase transition to the NNN phase at higher temperatures. Thus, it is not a mere coincidence that the two NN oriented structures (2a and 2b) are found to be stable at the low temperatures studied and the non-NN oriented structures (2c and 2d), although low in energy, do not survive for long times and eventually get destroyed. The two non-NN oriented structures were run at higher temperatures to test if they could be stabilized near room temperature but it always resulted in the loss of structure due to randomization of backbone orientations. This randomization of chain orientations at higher temperatures could be a result of the united atom potentials not being sufficiently repulsive. It is also possible that the having explicit hydrogens instead of the united atom approximation for the  $\text{CH}_x$  group might be crucial in order to stabilize these two structures. These two structures (2c and 2d) are considered strong candidates for the  $c(4 \times 2)$  superlattice as, apart from being low-energy structures, they display the surface topology that resembles the STM pattern reported by Poirier and Tarlov.<sup>3</sup> The desired topological pattern for both these structures can be

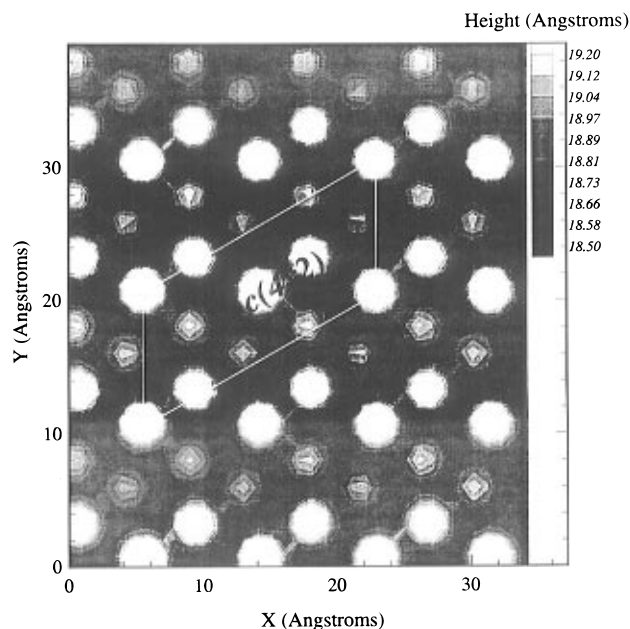


**Figure 4.** Computed topological picture of structure c showing the repeat pattern of bright and dark spots forming the  $c(4 \times 2)$  superlattice.

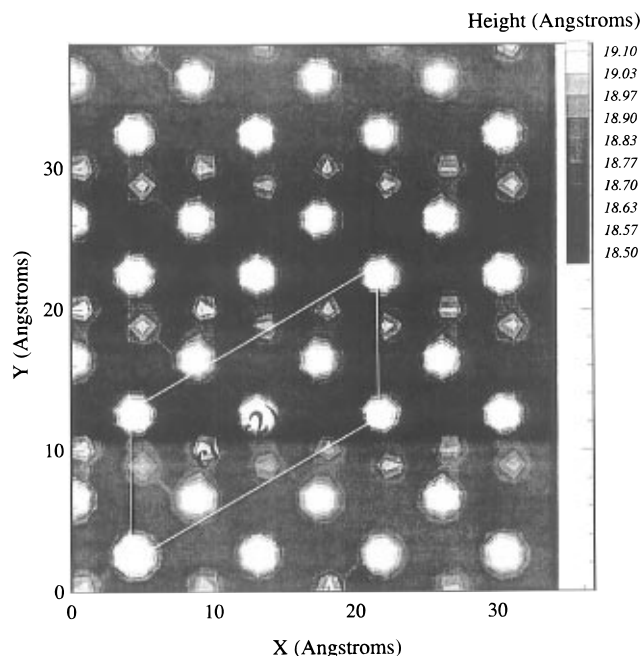


**Figure 5.** Computed topological picture of structure d showing the repeat pattern of bright and dark spots forming the  $c(4 \times 2)$  superlattice.

observed all along the MD run until the carbon backbones reorient so as to lose the structure. Parts c and d of Figure 2 are instantaneous snapshots, as short survival times make it difficult to get an average picture. Figure 4 and Figure 5 show the topologies computed for an instantaneous configuration of structures 2c and 2d, respectively.

Although structures 2a and 2b do not exhibit the desired STM topology at temperatures less than 100 K, it is possible that they may do so when heated. At higher temperatures, the tilt direction is expected to move away from the NN direction as it slowly undergoes a phase transition.<sup>13</sup> Unfortunately, the united atom method is not repulsive enough to stabilize a given configuration at room temperature and always lets the orientations of the backbones randomize under these conditions making it difficult to obtain the exact tilt direction at higher

temperatures. Our earlier work has shown that the chains would prefer to tilt toward one of the NNN directions, but the herringbone arrangement of the two kinds of chains might cause some steric hindrance allowing them to deviate slightly from this preferred direction.

Structure 2b is uniquely different from the rest of the proposed structures in that the two kinds of chains prefer to have two different tilt directions. Although the initial configuration consisted of all chains tilting in one common direction, the chains chose to rearrange in this manner. This structure is found to be stable only for very short chains ( $n = 4, 6$ ) as an increase in chain length makes it more difficult for the two kinds of chains to assume two different tilt directions in lieu of increased steric hindrance. This structure is lost at slightly lower temperatures as compared to 120 K for structure 2a, and this is because there is less room for thermal vibrations due to the two kinds of chains tilting in two different directions.

### Discussion

For a given chain length and temperature, there exists a complex interplay of the azimuthal tilt direction, the polar tilt angle with respect to the surface normal, and the relative orientation of the carbon backbones of the two kinds of chains. For example, part of the reason why structures 2a, 2b, and 2c settle for slightly different relative orientations between backbones is that the reorientation of backbones can facilitate the tilting of chains in the chosen azimuthal tilt direction (and vice versa). Other evidence for the interplay is provided by the fact that the polar tilt angle is affected by and affects the azimuthal tilt direction. We say this because identical initial configurations with different initial directions of tilt often seemed to favor different polar tilt angles. This is because the orientation of the carbon backbones can either favor or inhibit the chains tilting in a given direction (and vice versa). In fact, in structure 2c, that is one reason why the structure shows the high and low regions in the computed topological pattern. The chains tilting along the backbone direction (or close to it) are able to tilt less resulting in chains that are high where as those that are oriented away from that direction are able to tilt more resulting in chains that are low. At this point, it is appropriate to bring in the two regimes of structures observed by Fenter and Eisenberger<sup>10</sup> to attention. They observe a tilt angle of  $\sim 34.5^\circ$  for  $10 \leq n \leq 14$ , and the values we calculate for structure 2d are close to it. Structure 2c exhibits a tilt angle closer to  $30^\circ$  and that corresponds to the observed values in the second regime ( $16 \leq n \leq 30$ ). So, although it is conceivable that the superlattice structure in the two

regimes is totally different; it is nevertheless possible that a change in chain length merely results in a different choice of tilt direction thus not affecting the relative orientation of the backbones significantly.

As is apparent from the four proposed configurations, the chains prefer to tilt in a direction that is opposed to the direction of the vectors. This prevents the methylene adjacent to the sulfur atom from coming too close to the gold substrate. The chain backbone can also twist in such a way that the first methylene moves farther away from the substrate.

We also notice an interesting dynamical feature about these monolayers. All the structures that were unstable and ultimately got destroyed, owing to reorientation of the chain backbones, very often involved some amount of untilting ( $1-5^\circ$ ) before the loss of structure took place. So, it seems that untilting might be a preferred mechanism for the monolayers to undergo structural changes. This is very useful in designing new films as one can prevent the chain backbones from reorienting simply by adding bulky groups that make it harder for the chains to untilt.

### Conclusion

Four unique structures for the  $c(4 \times 2)$  superlattice of different length alkanethiols on Au{111} have been proposed. These structures have distinctive characteristics from previously proposed models. Namely, the herringbone arrangement of adjacent chain backbones is not rigorously perpendicular. Although it is impossible to decide which of the structures is absolutely correct, this study provides us with some useful insights that aid in the understanding of various factors that play a role in the determination of the structure of an organic film. It is our hope that more experiments will be designed to test these structures. From a theoretical vantage, we are currently incorporating potentials that include explicit H atoms into our code to refine the list of possible structures of the  $c(4 \times 2)$  superlattice.

**Acknowledgment.** We thank G. Scoles, P. Fenter, P. Weiss, G. Poirier, C. Chidsey, D. L. Allara, G. Gaynor, L. Zhigilei, R. Mahaffy, D. Srivastava, and K. Krom for invaluable discussions. The support of the National Science Foundation through the Chemistry Division, the GRT Program, and the CRIF program are gratefully acknowledged. Computational facilities were provided by the Selected University Research Program of the IBM Corporation and the Center for Academic Computing at the Pennsylvania State University.

LA962055D